

Nature of the LHCb pentaquarks from an analysis of the J/ψ p spectrum

Vadim Baru

Institut für Theoretische Physik II, Ruhr-Universität Bochum Germany

ITEP, Moscow, Russia

16th International Workshop on Meson Physics

18 May 2021

in collaboration with

M. Du, F.-K. Guo, C. Hanhart, U.-G. Meißner, J.A. Oller and Q. Wang

PRL 14, 072001 (2020) and arXiv: 2102.07159 (2021)

P_c 's from $\Lambda_b \rightarrow K J/\psi p$

LHCb Run-1 2015: one broad $P_c(4380)$ and one narrow $P_c(4450)$ state

LHCb, PRL 115 072001 (2015), PRL 117 082002 (2016)

P_c 's decay strongly into $J/\psi p \rightarrow$ quark content $c\bar{c}uud$

LHCb Run-2 2019:

LHCb, PRL 122 222001 (2019)

– order of magnitude larger statistics

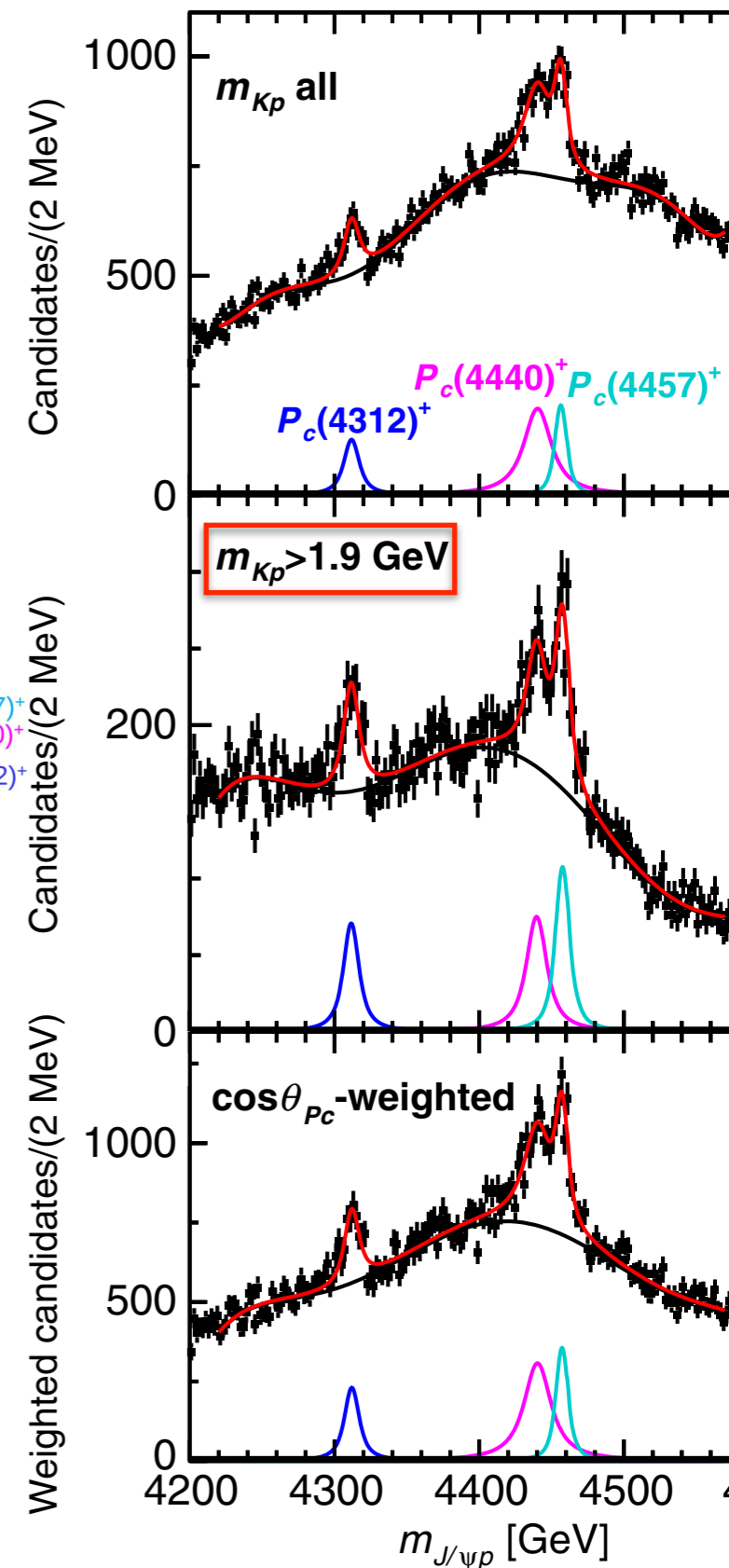
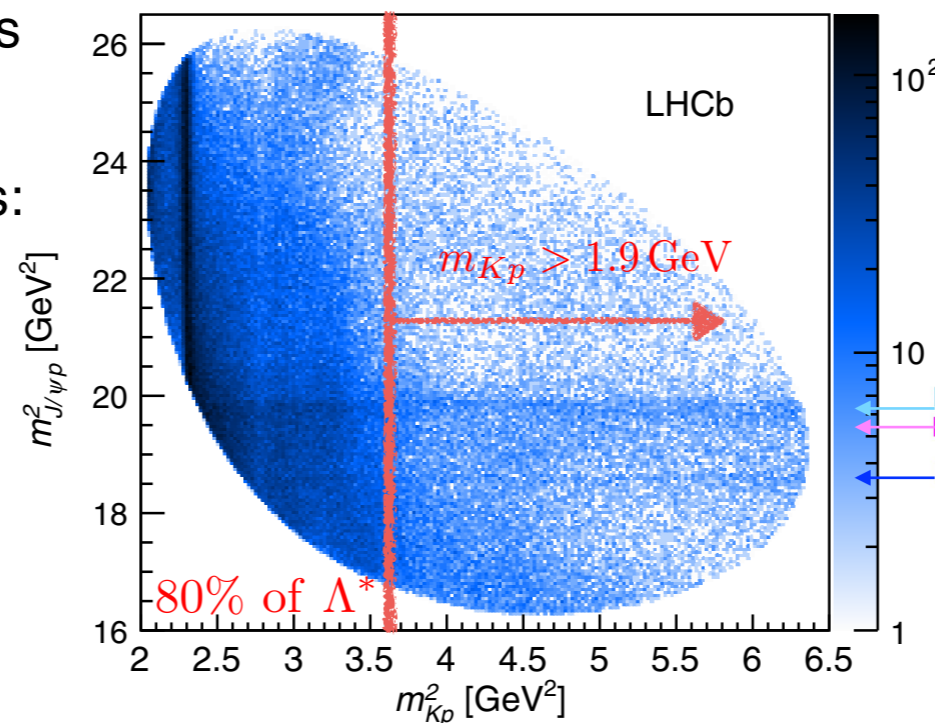
– samples with kinematic constraints:

\Rightarrow suppress $\Lambda^* \rightarrow Kp$

– New $P_c(4312)$ state

– $P_c(4450)$ split into two states

– Significance of a broad state dropped



State	M [MeV]	Γ [MeV]	(95% C.L.)	\mathcal{R} [%]
$P_c(4312)^+$	$4311.9 \pm 0.7^{+6.8}_{-0.6}$	$9.8 \pm 2.7^{+3.7}_{-4.5}$	(<27)	$0.30 \pm 0.07^{+0.34}_{-0.09}$
$P_c(4440)^+$	$4440.3 \pm 1.3^{+4.1}_{-4.7}$	$20.6 \pm 4.9^{+8.7}_{-10.1}$	(<49)	$1.11 \pm 0.33^{+0.22}_{-0.10}$
$P_c(4457)^+$	$4457.3 \pm 0.6^{+4.1}_{-1.7}$	$6.4 \pm 2.0^{+5.7}_{-1.9}$	(<20)	$0.53 \pm 0.16^{+0.15}_{-0.13}$

Pentaquarks as hadronic molecules

Disclaimer: I will not talk about P_c 's as compact states, hadrocharmonia, triangle mechanisms...

Brambilla et al *Phys.Rept.* 873 (2020) 1

— All P_c 's reside near S-wave hadronic thresholds:

$P_c(4312)$ — near $\Sigma_c D$, $P_c(4440)$ and $P_c(4457)$ — near $\Sigma_c D^*$

⇒ Hint for a molecular scenario

⇒ Implications of QCD symmetries:

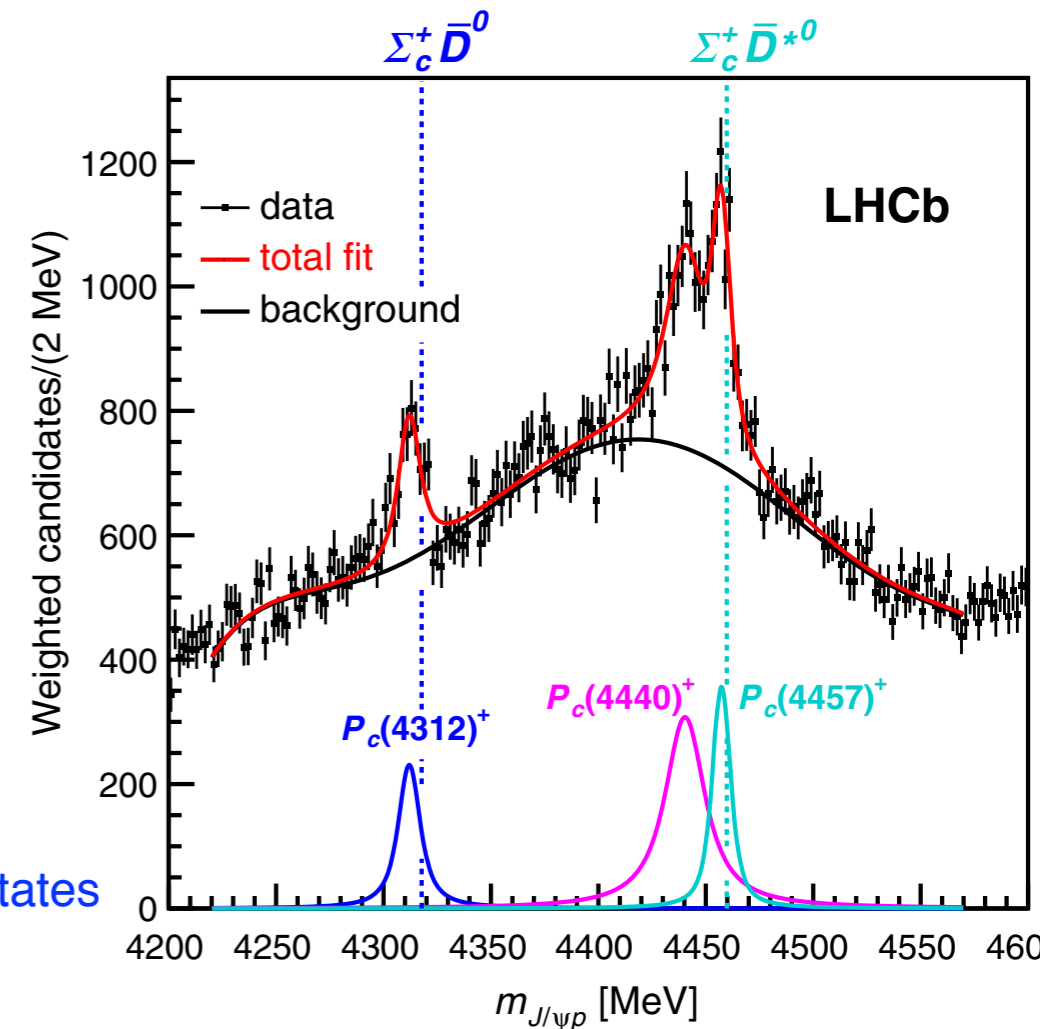
— chiral symmetry: one- and multi-pion exchanges

— heavy-quark spin symmetry (HQSS): there must be seven $\Sigma_c^{(*)} \bar{D}^{(*)}$ states

$$\mathcal{L}_{\text{LO}} = \underbrace{-C_a \mathbf{S}_{ab}^\dagger \cdot \mathbf{S}_{ba} \langle \bar{H}_c^\dagger \bar{H}_c \rangle}_{\text{central}} - \underbrace{C_b i \epsilon_{jik} S_{ab}^{j\dagger} S_{ba}^k \langle \bar{H}_c^\dagger \sigma^i \bar{H}_c \rangle}_{\text{spin-spin}}$$

⇒ First predictions for spin partners using masses of $P_c(4312)$, $P_c(4440)$ and $P_c(4457)$ as input and neglecting coupled-channels

Liu et al, PRL 122 242001 (2019)

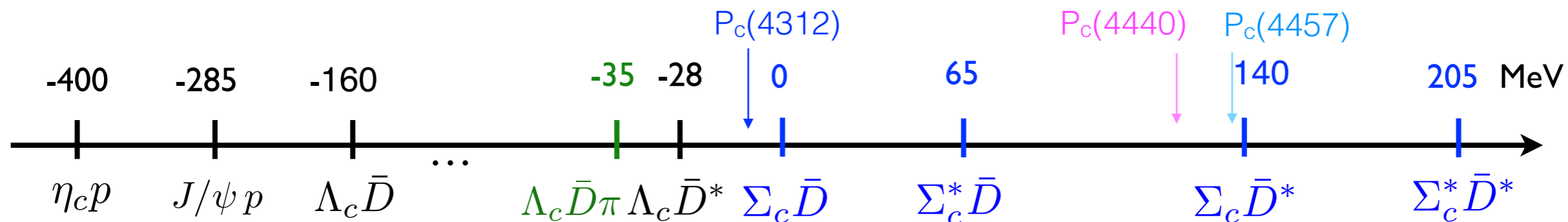


LHCb, PRL 122 222001 (2019)

This Talk is about

our works: PRL 14, 072001 (2020) and arXiv: 2102.07159 (2021)

- A coupled-channel analysis of the LHCb spectra using an EFT approach



- Fixing LECs from data and not from Breit-Wigner masses, as done before
 \implies extracting poles and residues

- Parameter-free testable predictions for HQSS partners and line shapes in

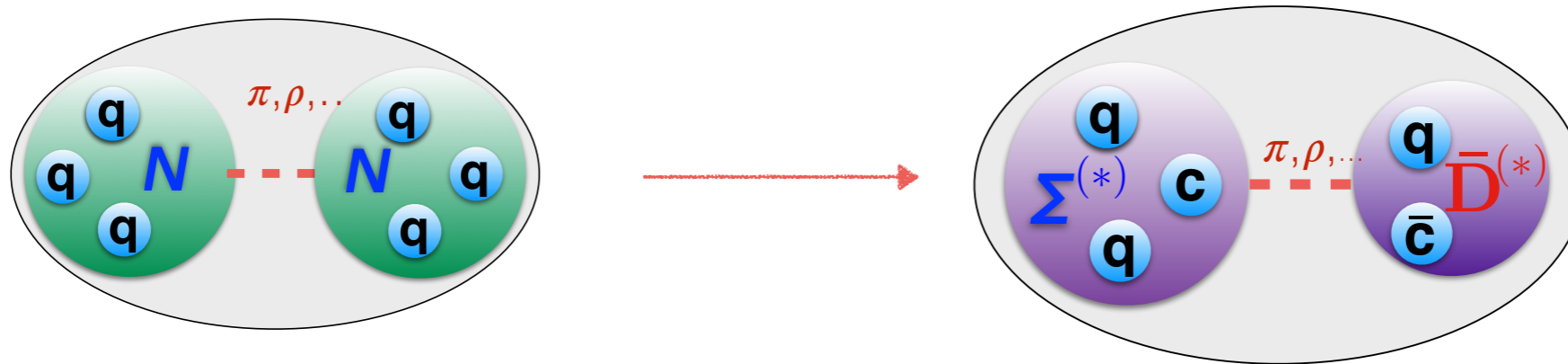
$$\Lambda_b \rightarrow K \Sigma^{(*)} \bar{D}^{(*)} \text{ and } \Lambda_b \rightarrow K \eta_c p$$

first data by LHCb for $\Lambda_b \rightarrow K \eta_c p$: PRD 102, 112012 (2020)

and for $\Lambda_b \rightarrow K \Lambda_c D$: Piucchi phd thesis (2019)

- The role of one-pion exchange

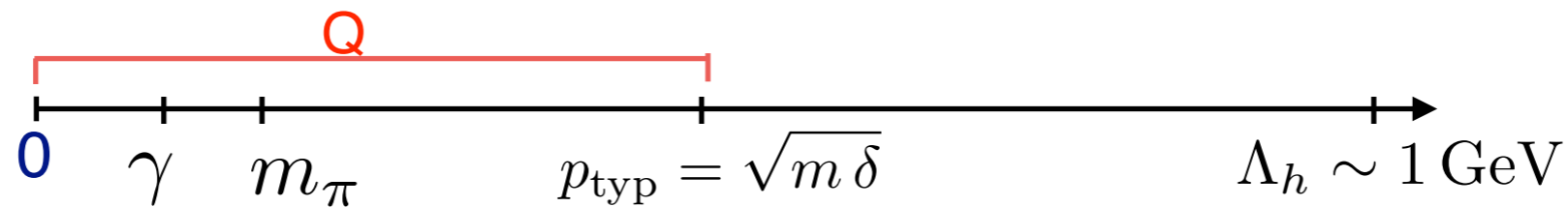
Chiral EFT approach at low energies



Voloshin, Okun (1976)

- Elastic coupled-channel $\Sigma_c^{(*)} \bar{D}^{(*)}$ potential to a given order in Q/Λ_h

➡ typical soft scale Q is quite large because of coupled-channels



➡ $V_{\text{LO}}^{\text{eff}} =$

HQSS: 2 S-S wave LECs at $O(Q^0)$
 1 S-D wave LEC at $O(Q^2)$

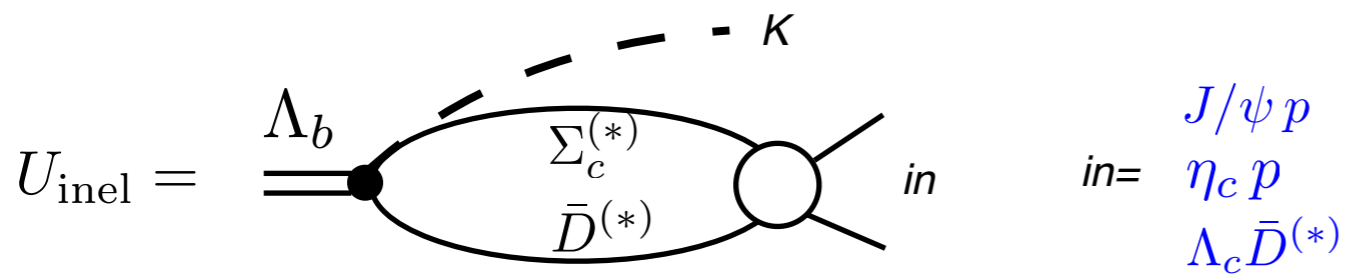
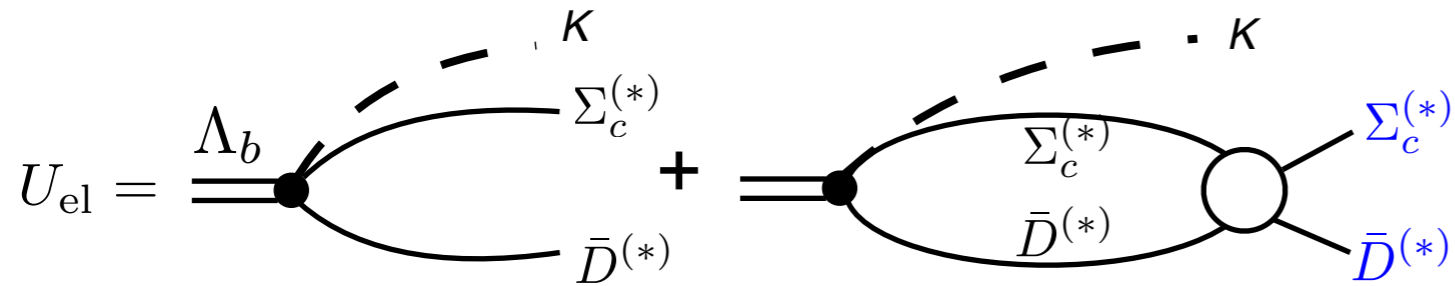
Long range: OPE

Imaginary part from inelastic channels

➡ If $\Sigma_c^{(*)} \bar{D}^{(*)} \rightarrow \Lambda_c \bar{D}^{(*)}$ are included, one more S-S and one S-D LECs plus OPE

Formalism: production and inelastic channels

— Weak production $\Lambda_b^0 \rightarrow K \Sigma_c^{(*)} D^{(*)}$
↑
7 states



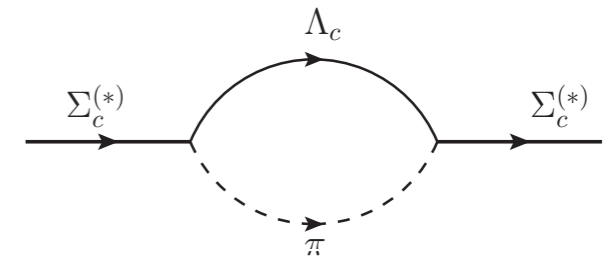
— No direct inelastic transitions
 — via couplings to elastic channels

$$T_{\alpha\beta} = V_{\alpha\beta}^{\text{eff}} - \sum_{\gamma} \int \frac{d^3q}{(2\pi)^3} V_{\alpha\gamma}^{\text{eff}} G_{\gamma} T_{\gamma\beta}$$

Green function:

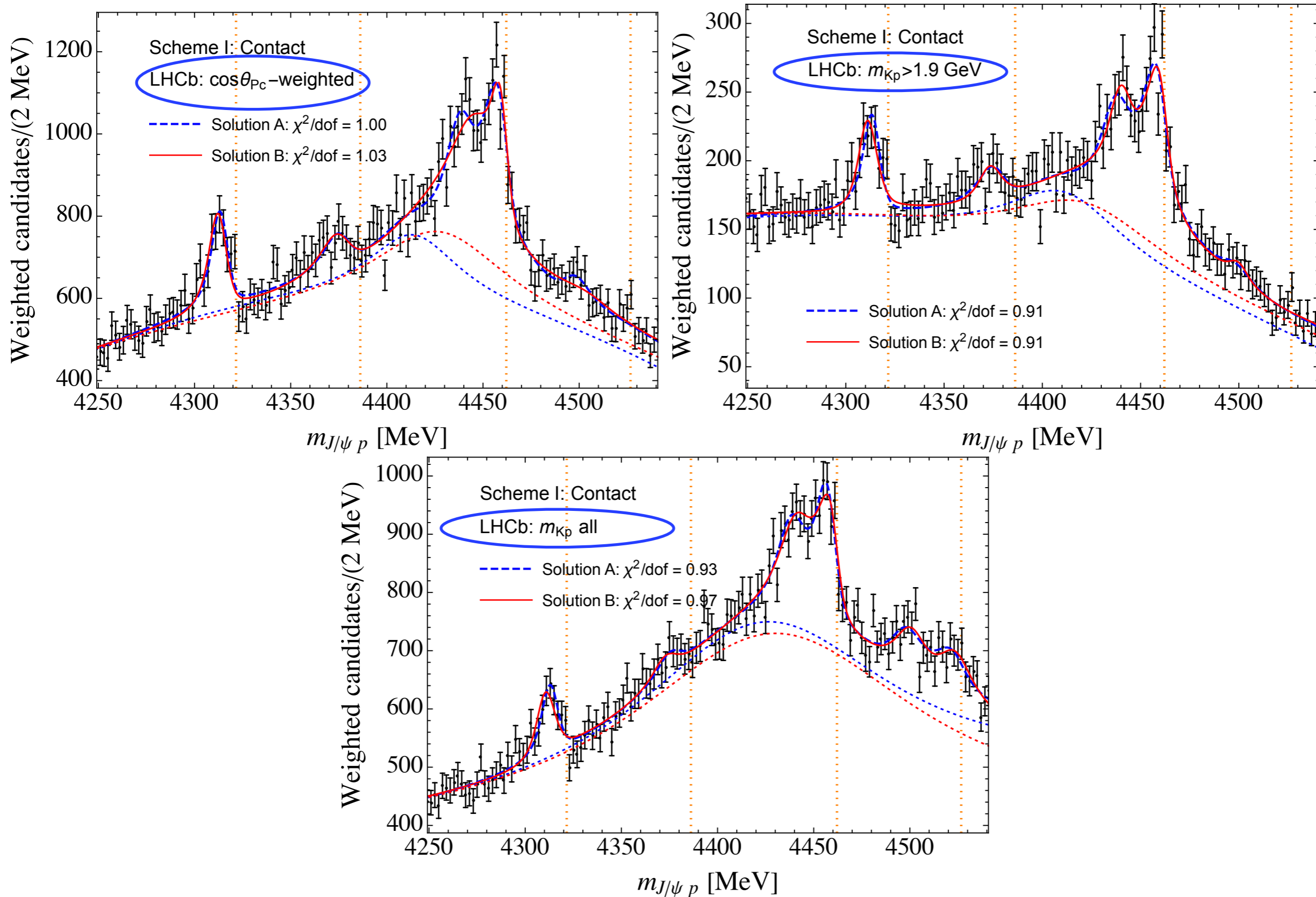
$$G_{\beta}(E, \mathbf{q}) = \frac{m_{\Sigma_c^{(*)}} m_{D^{(*)}}}{E_{\Sigma_c^{(*)}}(\mathbf{q}) E_{D^{(*)}}(\mathbf{q})} \frac{1}{E_{\Sigma_c^{(*)}}(\mathbf{q}) + E_{D^{(*)}}(\mathbf{q}) - E - \frac{\tilde{\Sigma}_R(s)}{2E_{\Sigma_c^{(*)}}(\mathbf{q})}}$$

— Dynamical widths of $\Sigma_c^{(*)}$



generates $\bar{D} \Lambda_c \pi$ cut

“Contact” Fits to three sets of LHCb data

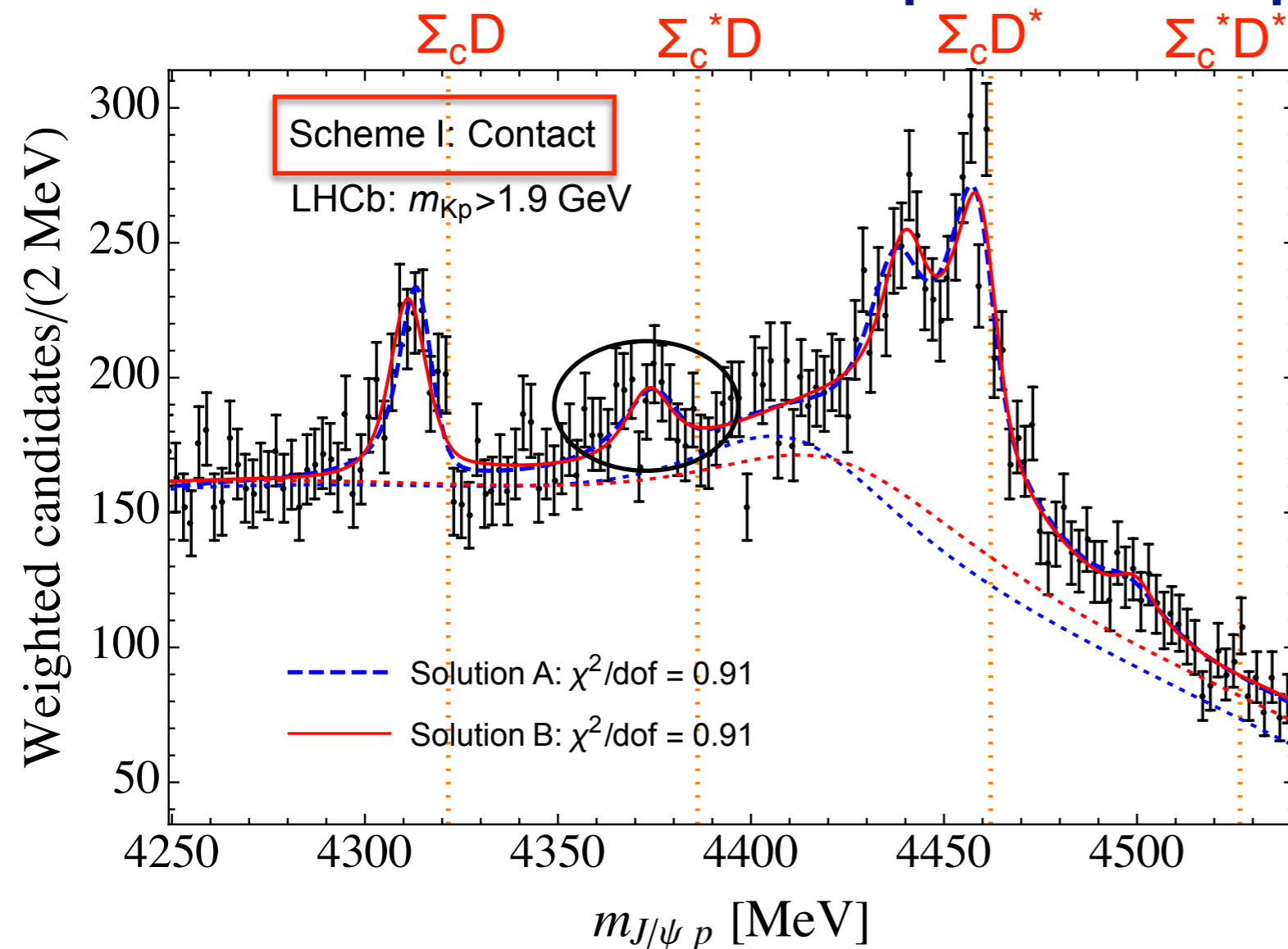


⇒ Consistent values for the P_c 's poles from all fits

Line shape and Pc poles

Du et al. PRL 124, 072001 (2020)

and arXiv:2102.07159



→ $P_c(4312)$, $P_c(4440)$, $P_c(4457)$ are well understood as $\Sigma_c D$, $\Sigma_c D^*$ and $\Sigma_c^* D^*$ quasi-bound states, respectively

→ Two fits with equal χ^2 yield:

	$P_c(4440)$	$P_c(4457)$
Fit A:	$1/2^-$	$3/2^-$
Fit B:	$3/2^-$	$1/2^-$

→ A narrow $P_c(4380)$ state predicted as a $\Sigma_c^* D$ $3/2^-$ molecule is seen in data

Poles and quantum numbers:

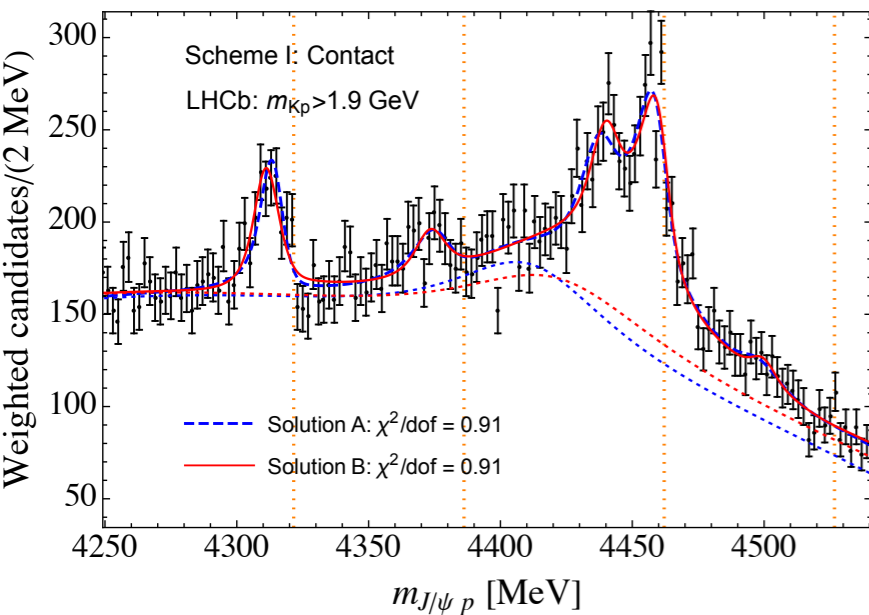
	thr. ([MeV])	solution A		solution B	
		J^P	Pole [MeV]	J^P	Pole [MeV]
$P_c(4312)$	$\Sigma_c \bar{D}$ (4321.6)	$\frac{1}{2}^-$	4314(1) - 4(1)i	$\frac{1}{2}^-$	4312(2) - 4(2)i
$P_c(4380)$	$\Sigma_c^* \bar{D}$ (4386.2)	$\frac{3}{2}^-$	4377(1) - 7(1)i	$\frac{3}{2}^-$	4375(2) - 6(1)i
$P_c(4440)$	$\Sigma_c \bar{D}^*$ (4462.1)	$\frac{1}{2}^-$	4440(1) - 9(2)i	$\frac{3}{2}^-$	4441(3) - 5(2)i
$P_c(4457)$	$\Sigma_c \bar{D}^*$ (4462.1)	$\frac{3}{2}^-$	4458(2) - 3(1)i	$\frac{1}{2}^-$	4462(4) - 5(3)i
P_c	$\Sigma_c^* \bar{D}^*$ (4526.7)	$\frac{1}{2}^-$	4498(2) - 9(3)i	$\frac{1}{2}^-$	4526(3) - 9(2)i
P_c	$\Sigma_c^* \bar{D}^*$ (4526.7)	$\frac{3}{2}^-$	4510(2) - 14(3)i	$\frac{3}{2}^-$	4521(2) - 12(3)i
P_c	$\Sigma_c^* \bar{D}^*$ (4526.7)	$\frac{5}{2}^-$	4525(2) - 9(3)i	$\frac{5}{2}^-$	4501(3) - 6(4)i

→ $\Sigma_c^* D^*$ states are not seen yet, their production rate is suppressed

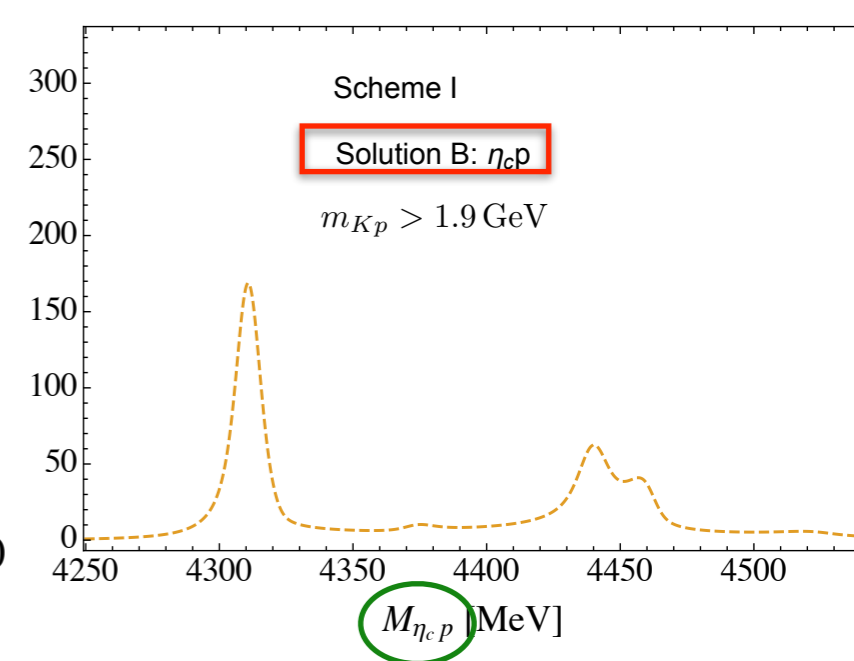
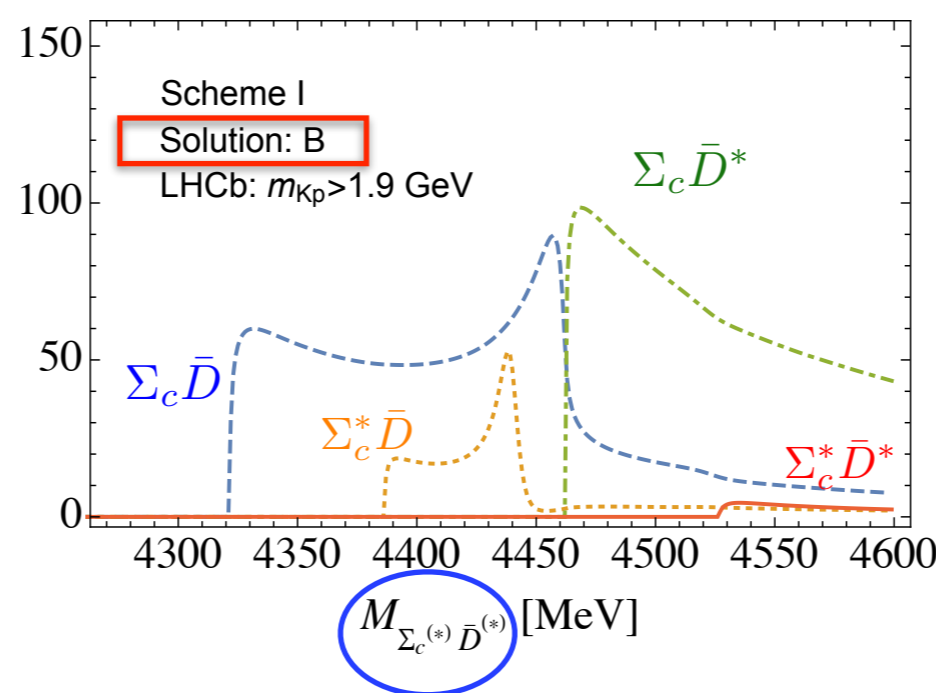
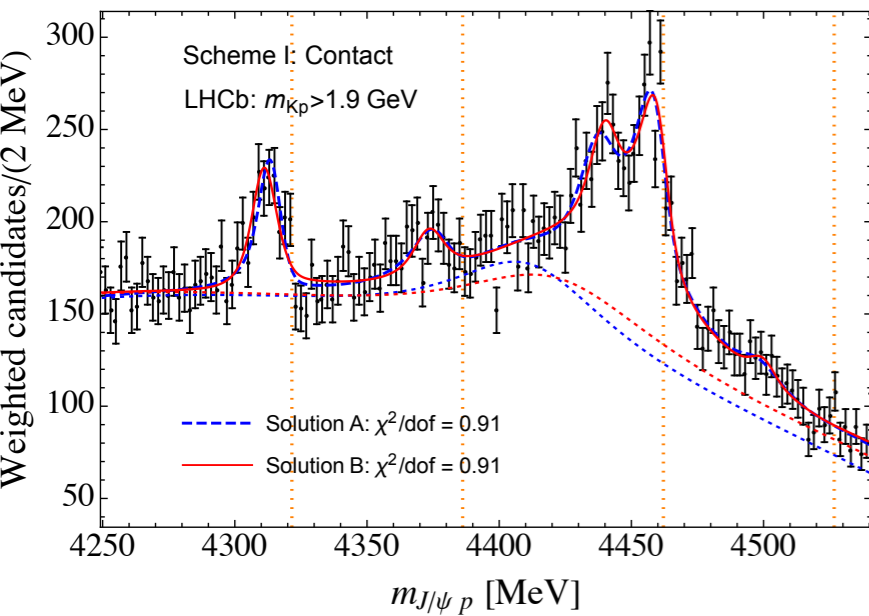
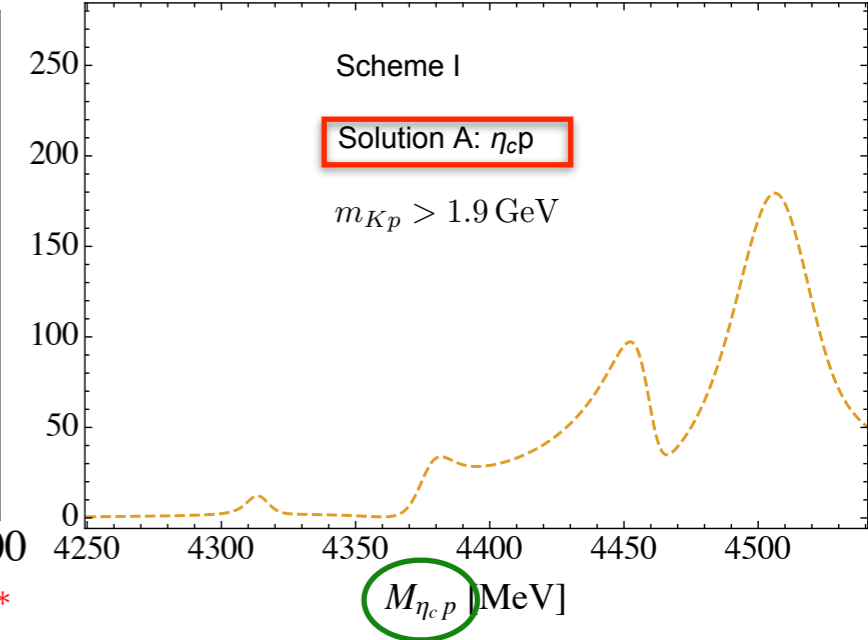
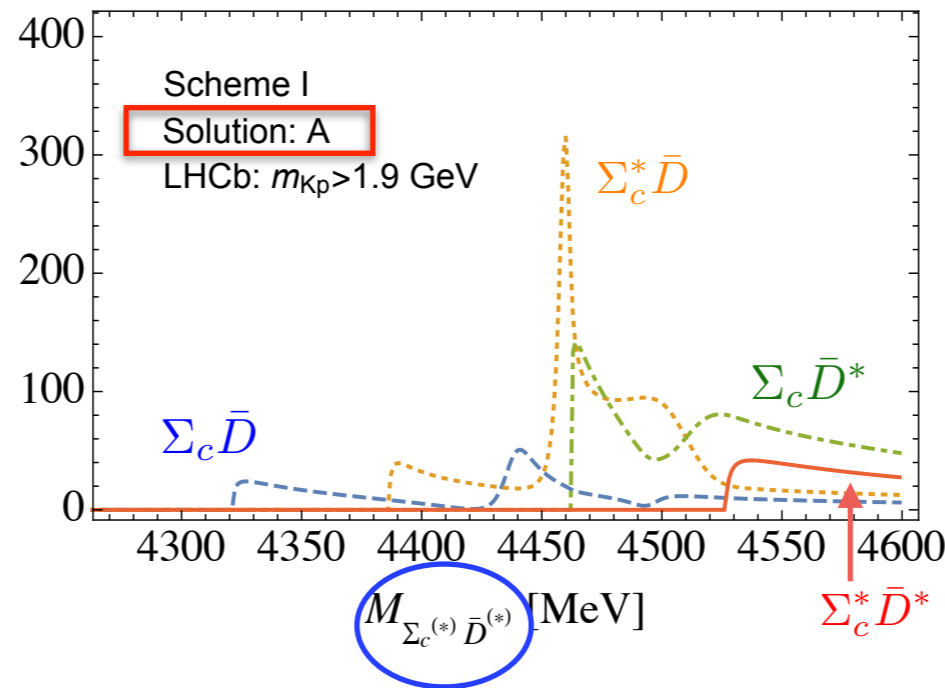
Predictions for $\Lambda_b \rightarrow K \Sigma^{(*)} D^{(*)}$ and $\Lambda_b \rightarrow K \eta_c p$

scheme I = contact

Fitted



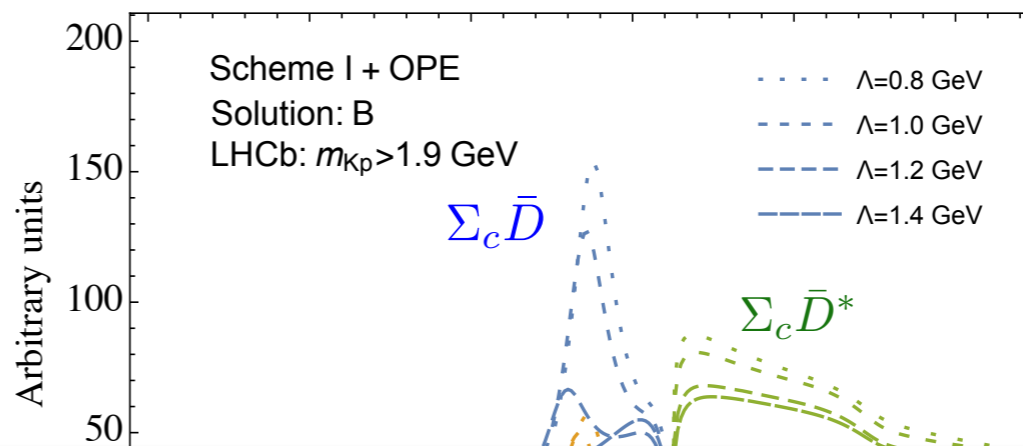
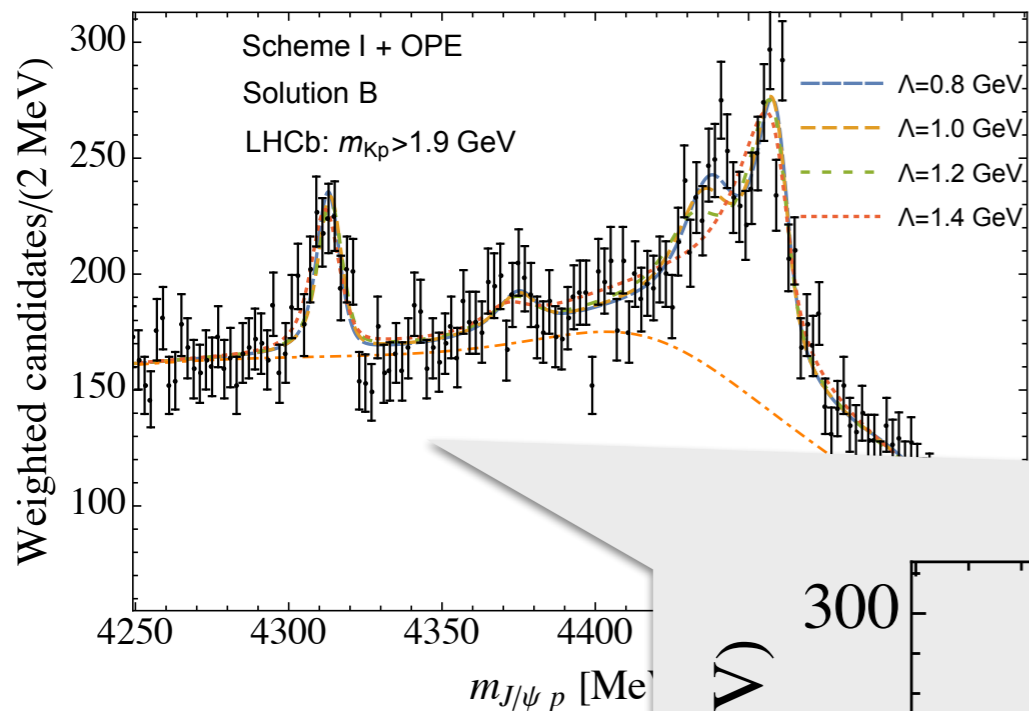
Predicted



- Very different predictions for fits A and B

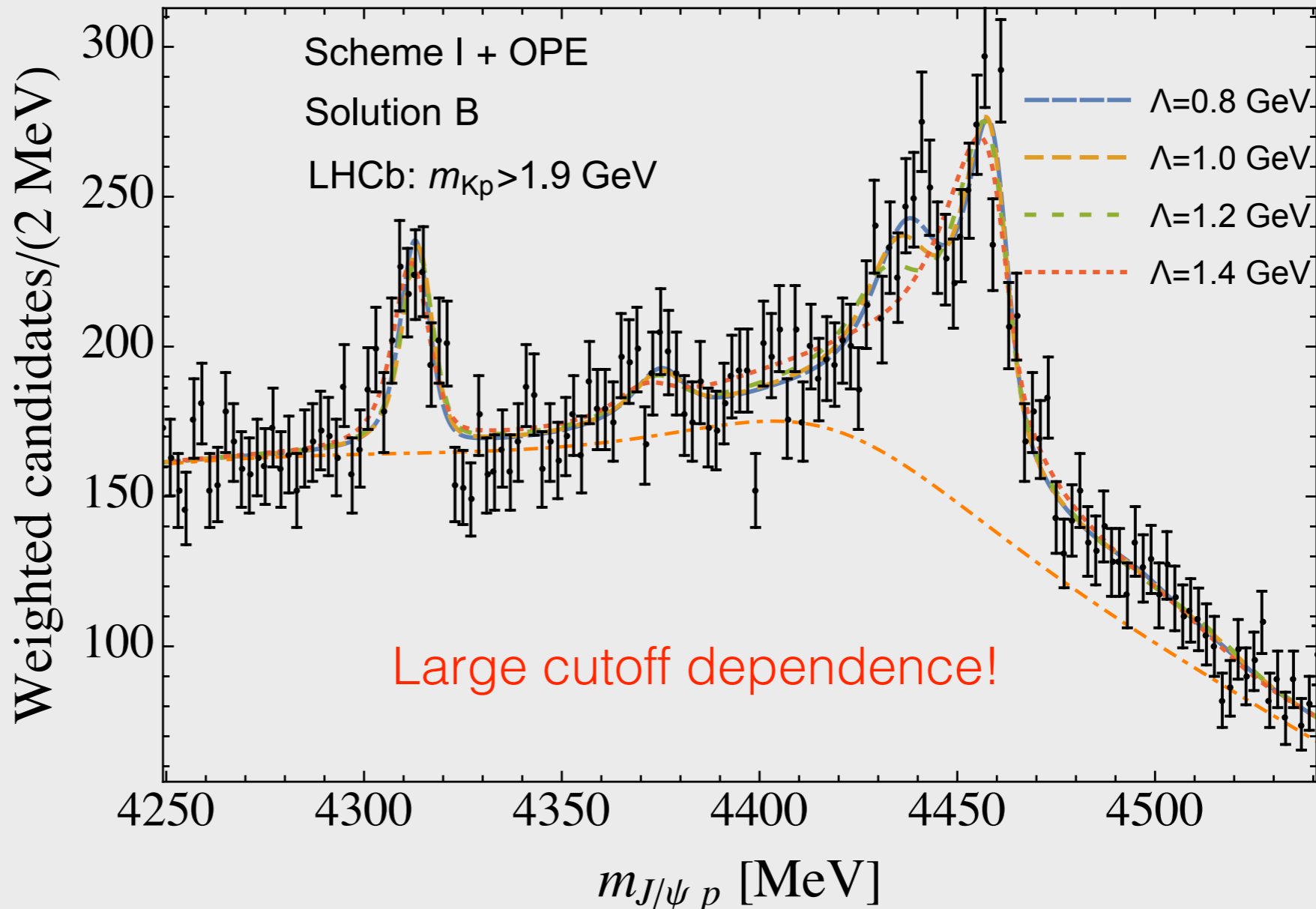
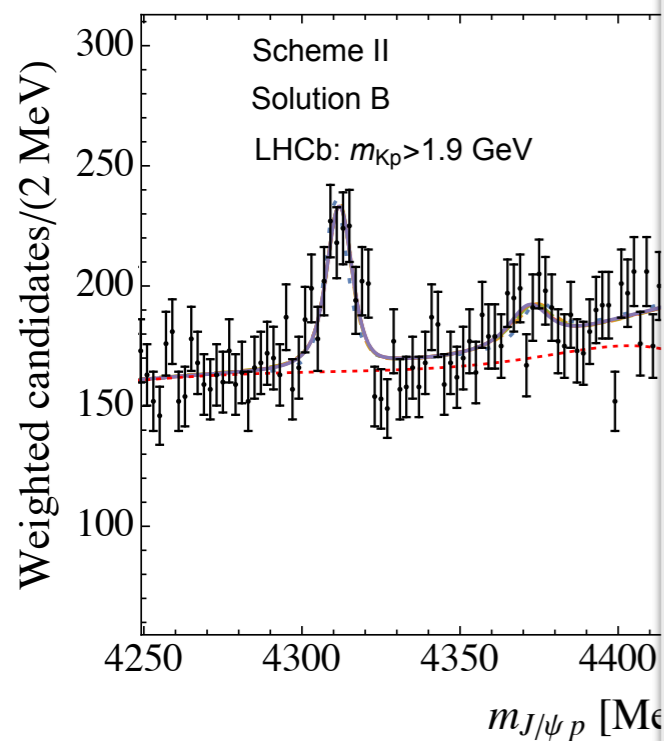
⇒ data in these channels will clearly distinguish between the two fits

But what happens if we include pions?



Without
S-wave—D-wave
contact term

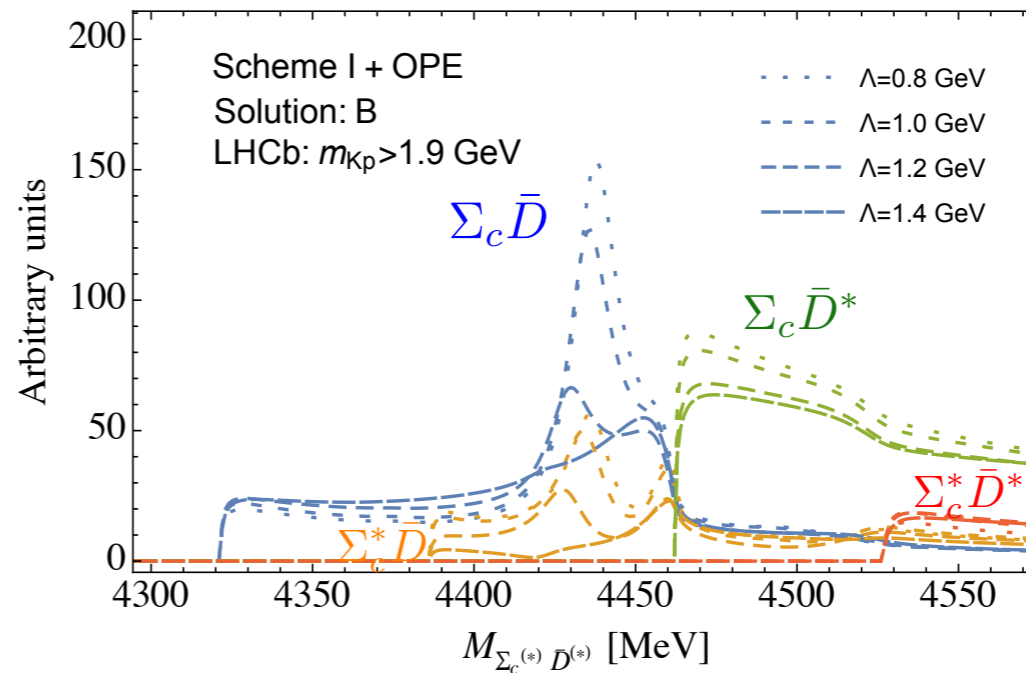
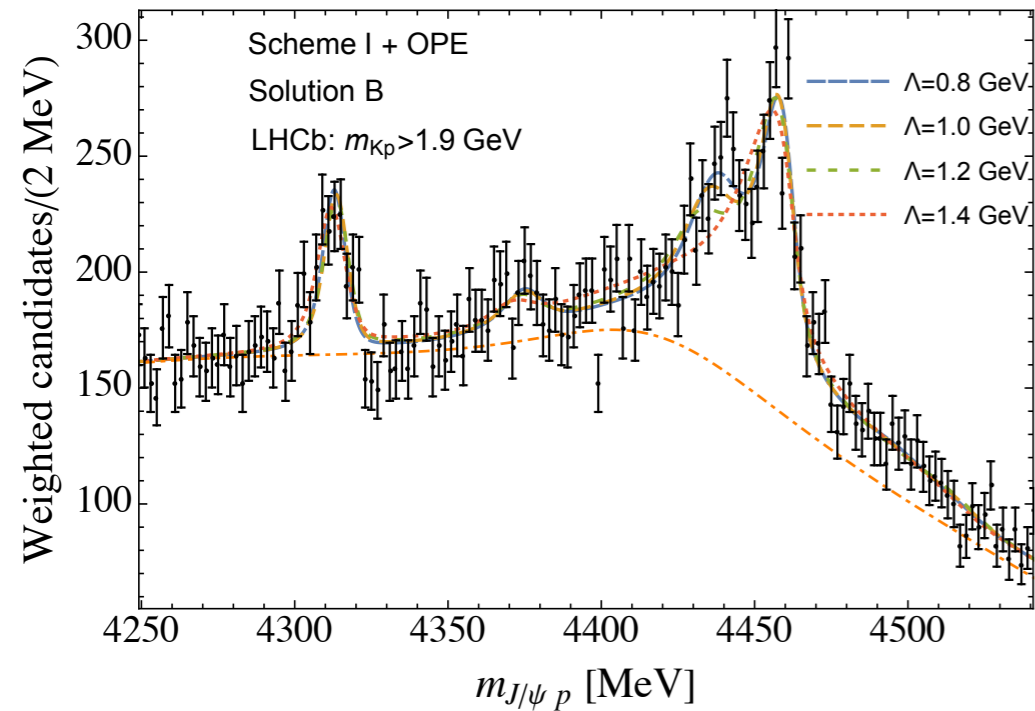
Large cutoff
dependence!



• Renormalizability

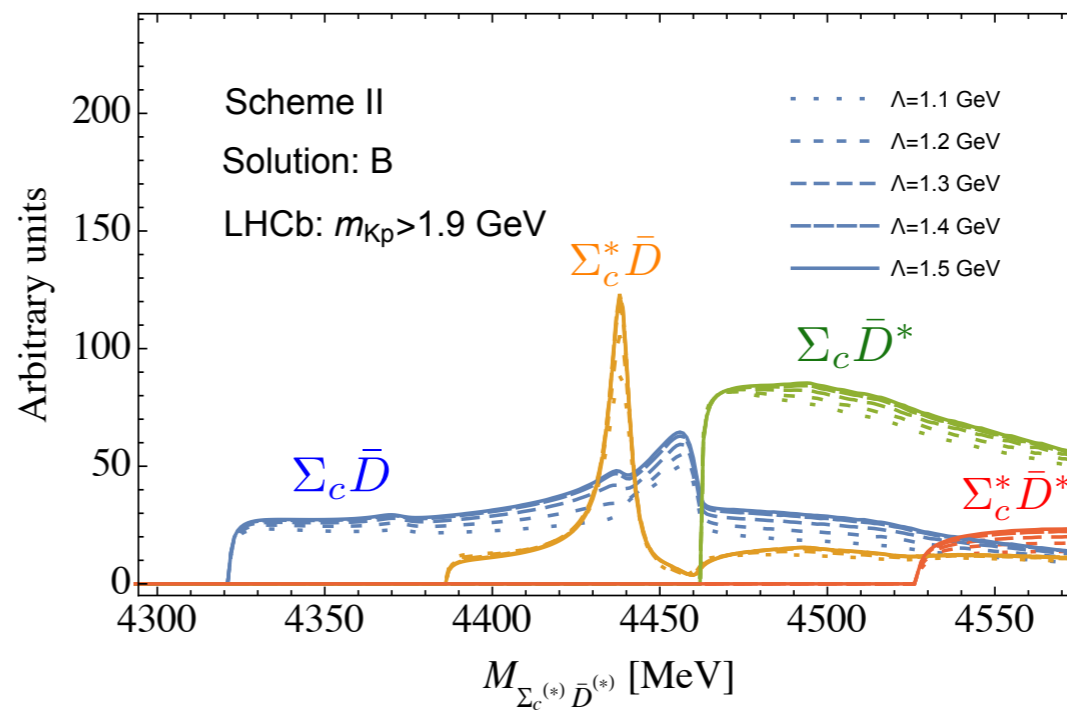
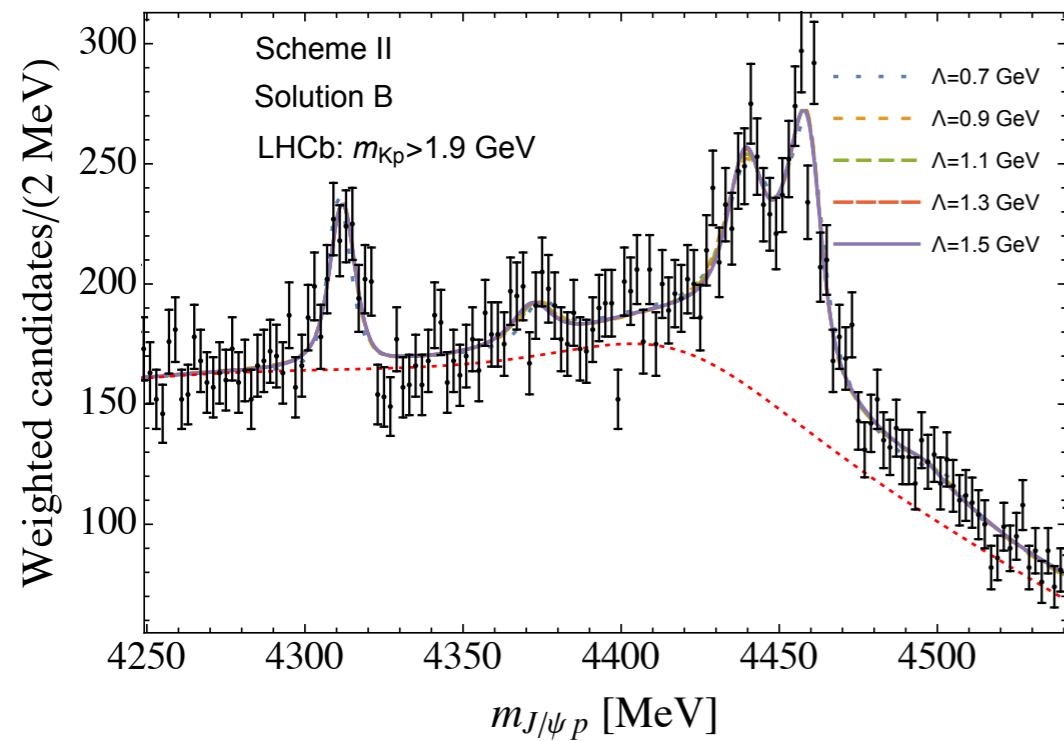
• completely consistent

But what happens if we include pions?



Without
S-wave—D-wave
contact term

Large cutoff
dependence!



With S-D
contact term

cutoff independent
results!

- Renormalizability require S-wave-to-D-wave contact term to appear together with OPE
- completely consistent with similar analyses of Zb(10610)/Zb(10650)

our works: PRD 98,074023 (2018),
PRD 99,094013 (2019)

Predictions for $\Lambda_b \rightarrow K \Sigma^{(*)} D^{(*)}$ and $\Lambda_b \rightarrow K \eta_c p$ with pions

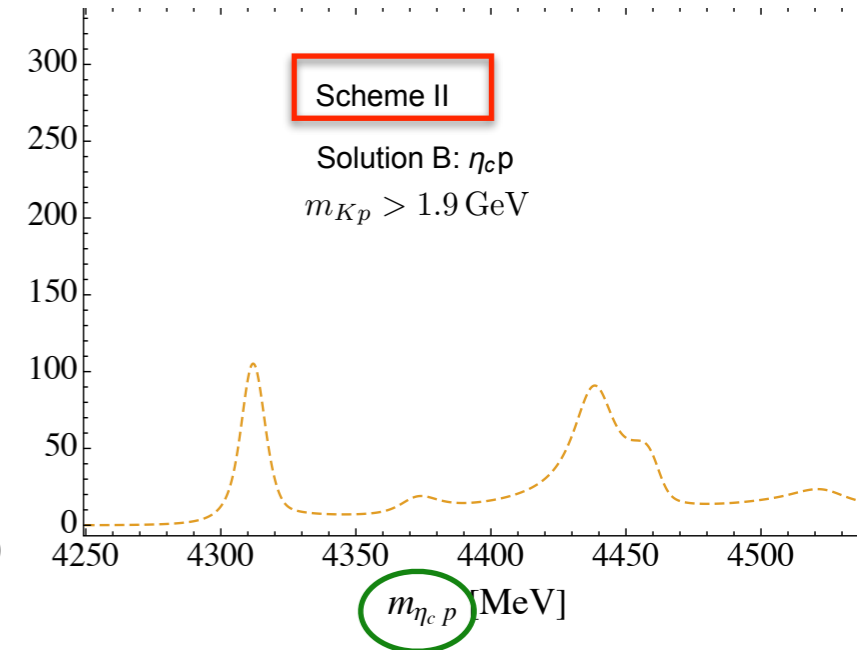
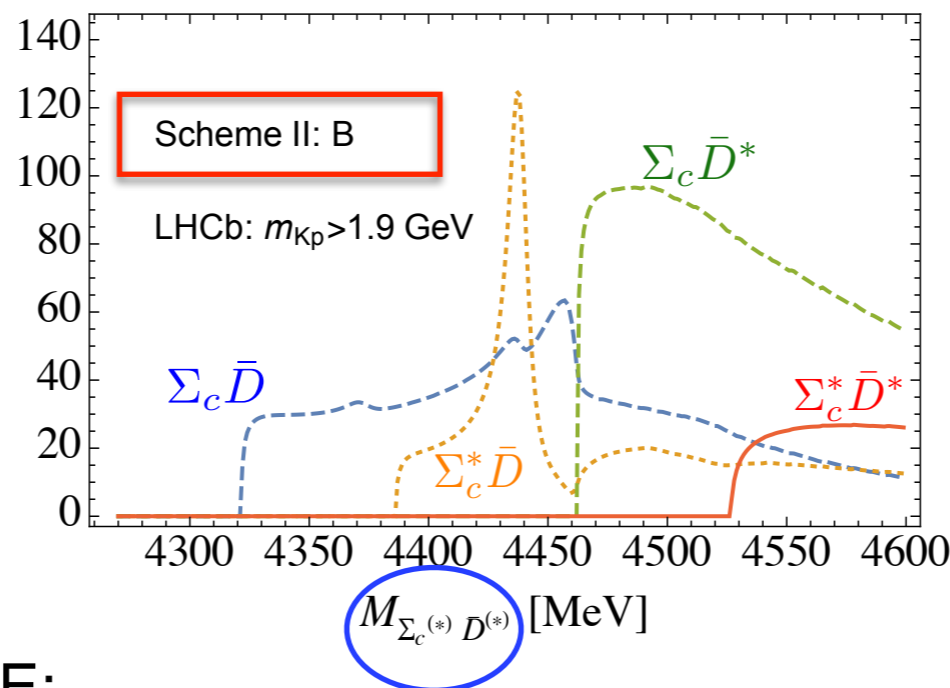
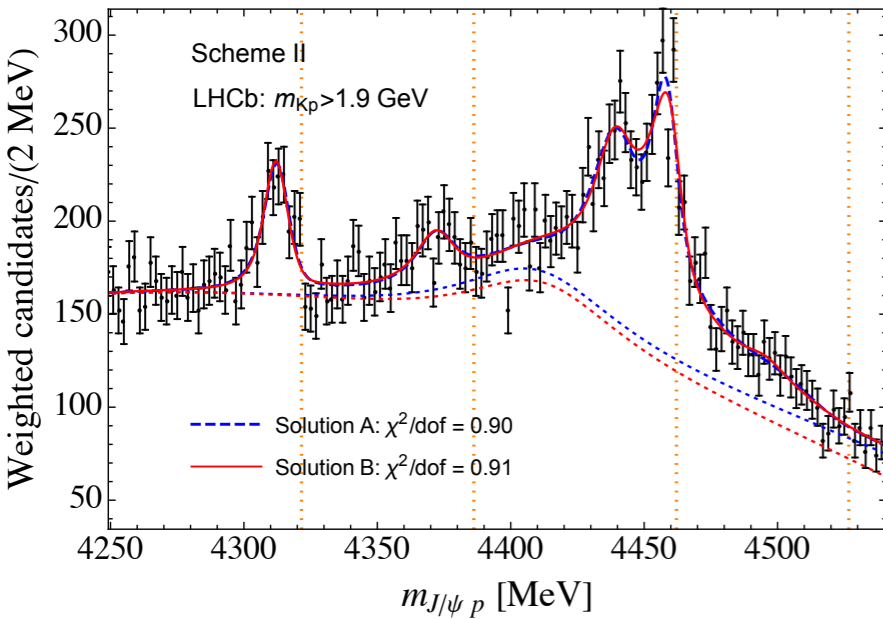
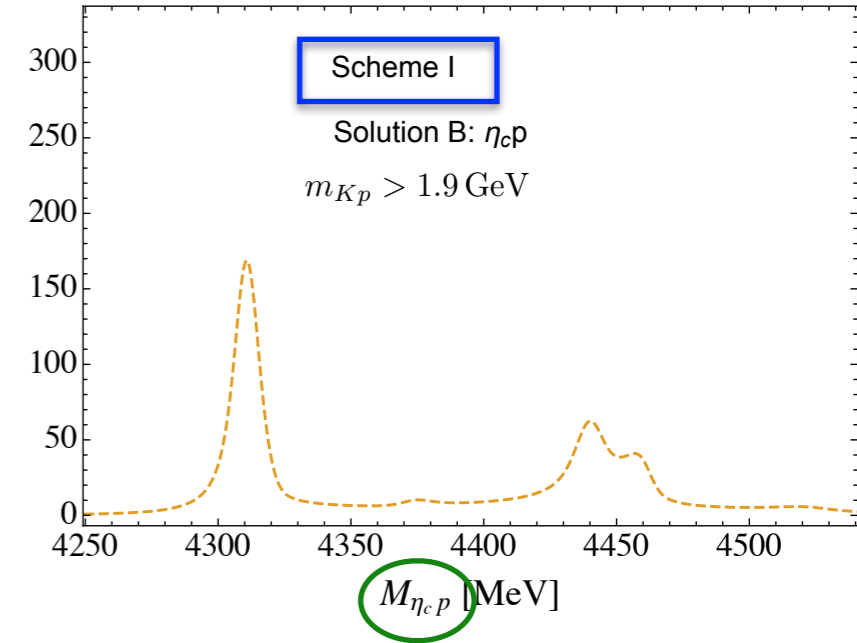
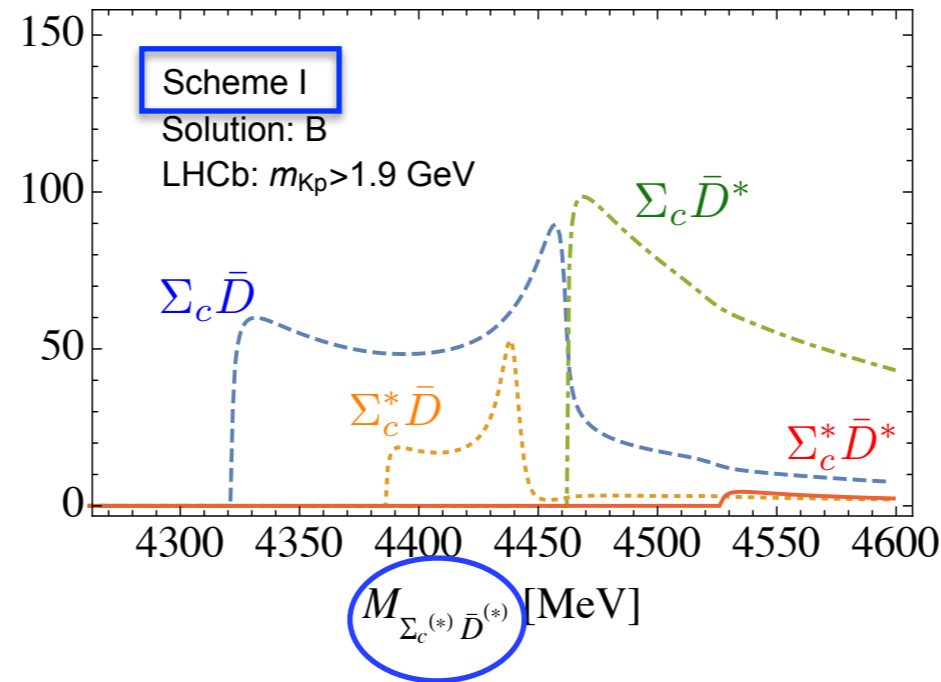
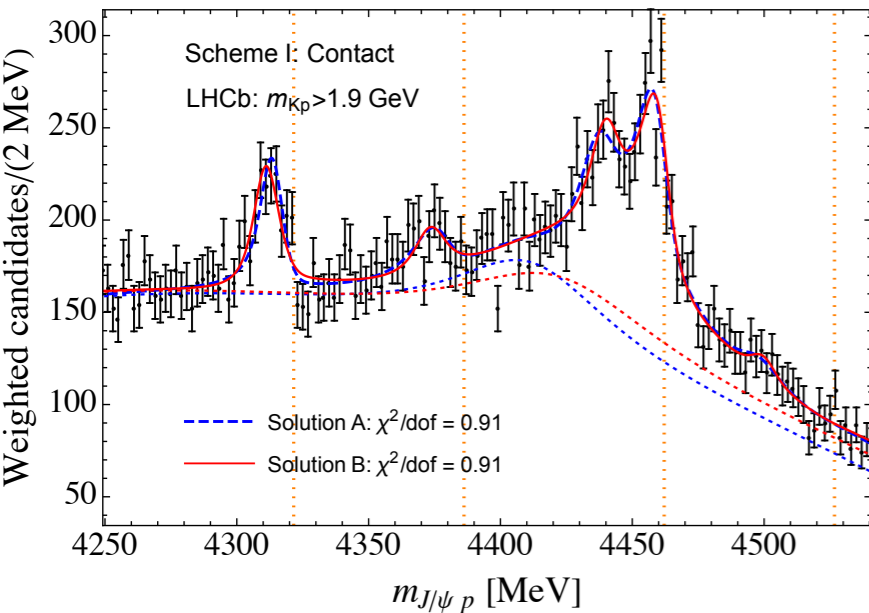
Fit B

scheme I = contact

scheme II = contact + OPE

Fitted

Predicted



The effect from renormalised OPE:

- Qualitatively similar results: the position of peaks is the same
- The inclusion of OPE has a visible impact on the peaks strength

Predictions for $\Lambda_b \rightarrow K \Sigma^{(*)} D^{(*)}$ and $\Lambda_b \rightarrow K \eta_c p$ with pions

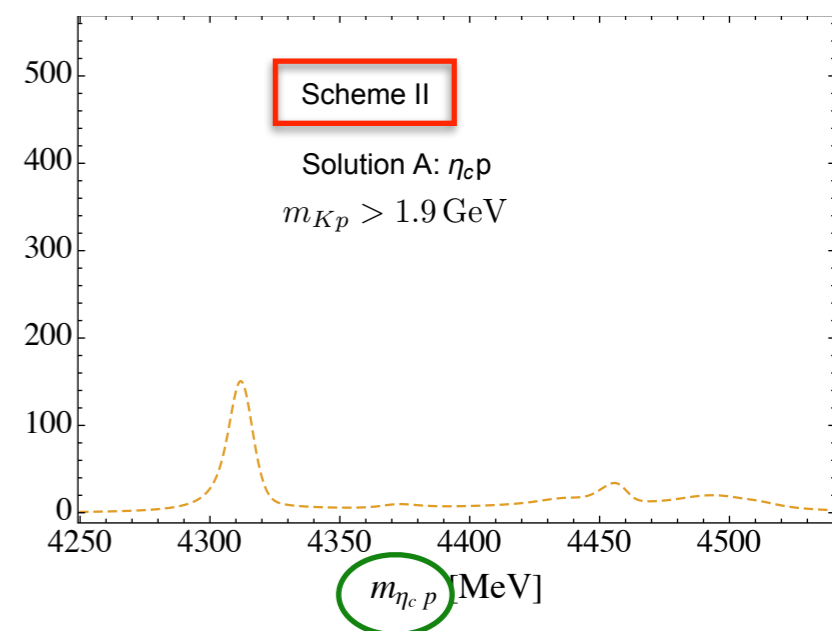
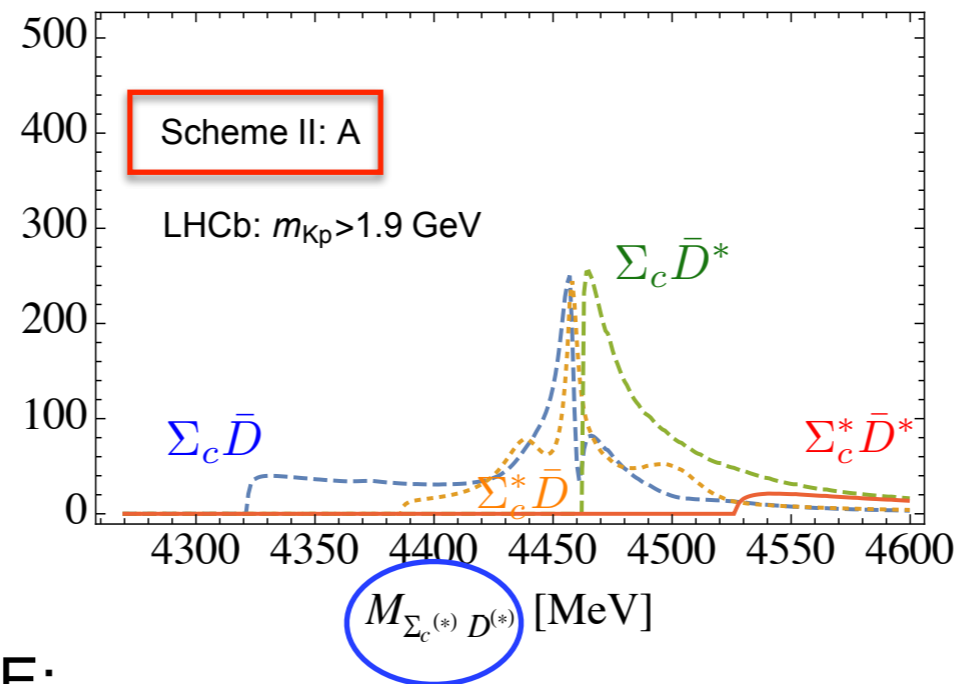
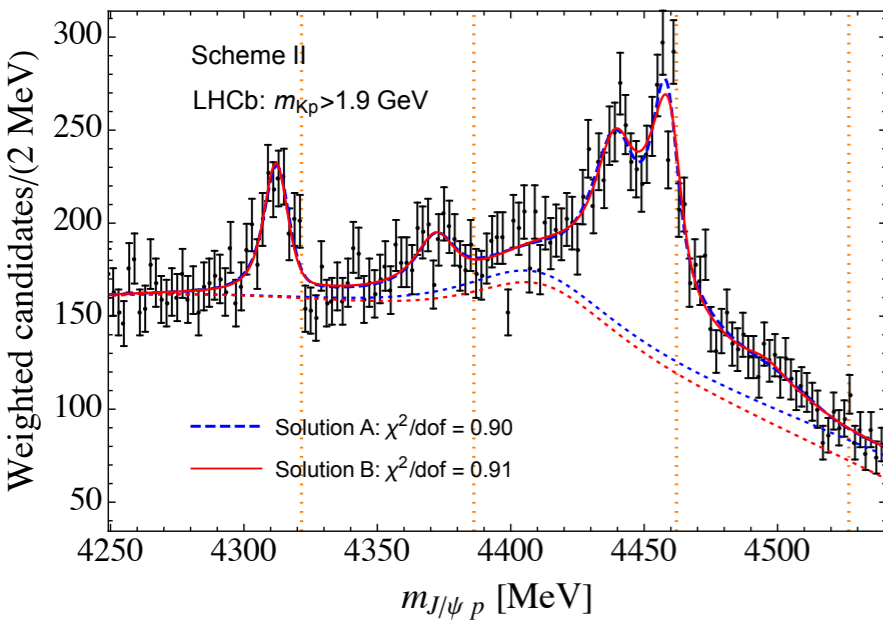
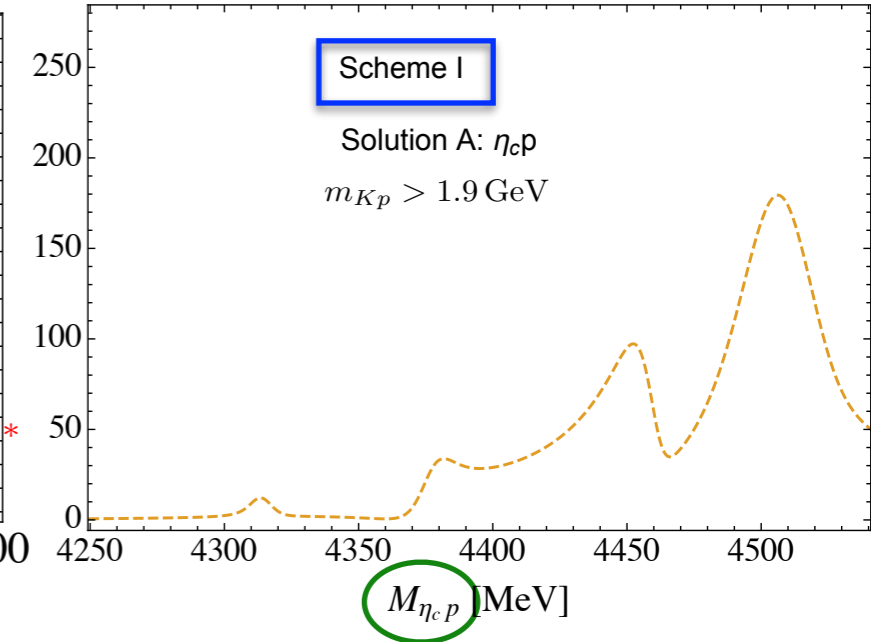
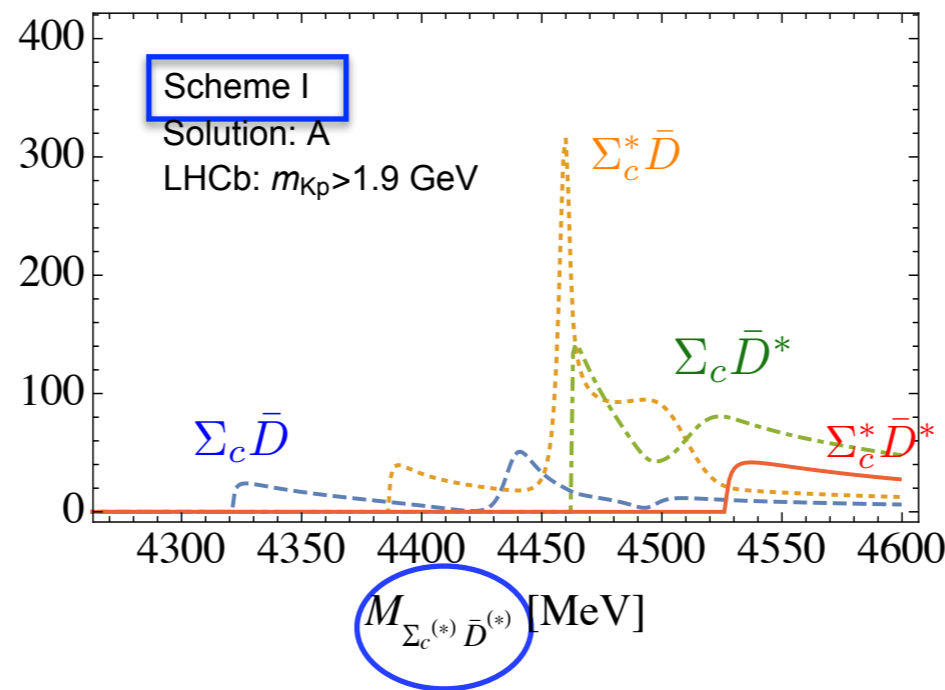
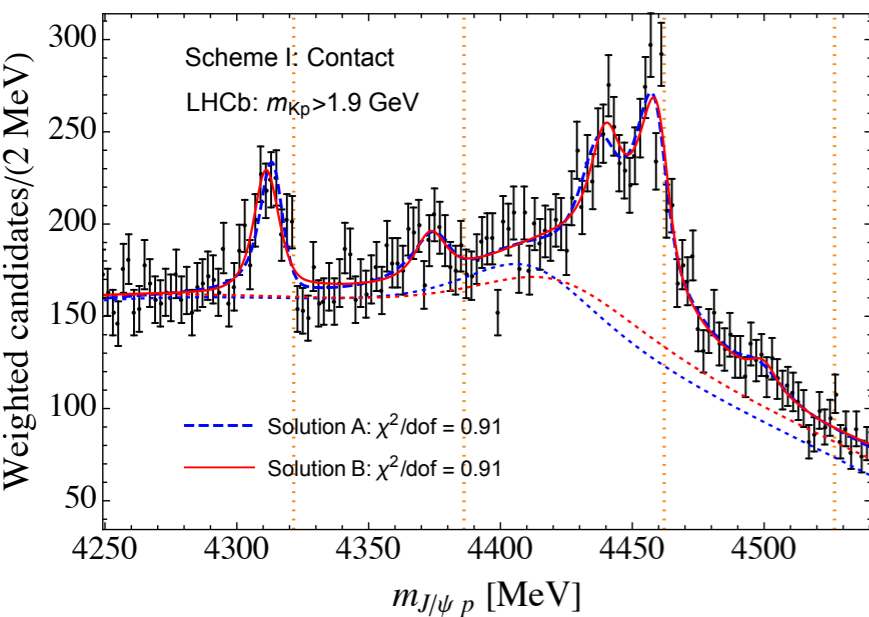
Fit A

scheme I = contact

scheme II = contact + OPE

Fitted

Predicted



The effect from renormalised OPE:

- Qualitatively different results for $\Sigma_c D$ and $\eta_c p$ in schemes I and II
- $\Sigma_c D$: 1/2- $P_c(4440)$ in S-wave in scheme I vs 3/2- $P_c(4457)$ in D-wave in scheme II

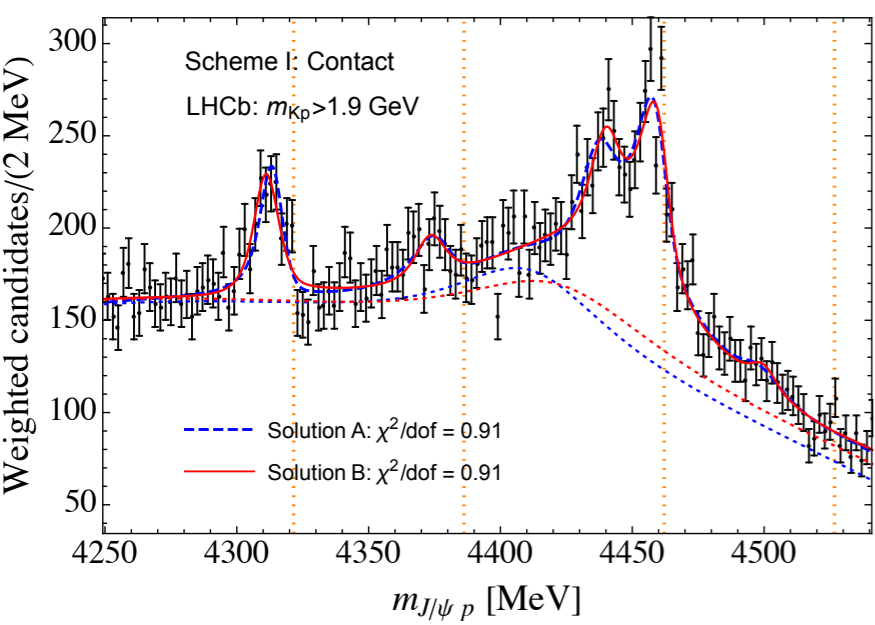
Predictions for $\Lambda_b \rightarrow K \Sigma^{(*)} D^{(*)}$ and $\Lambda_b \rightarrow K \eta_c p$ with pions

scheme I = contact

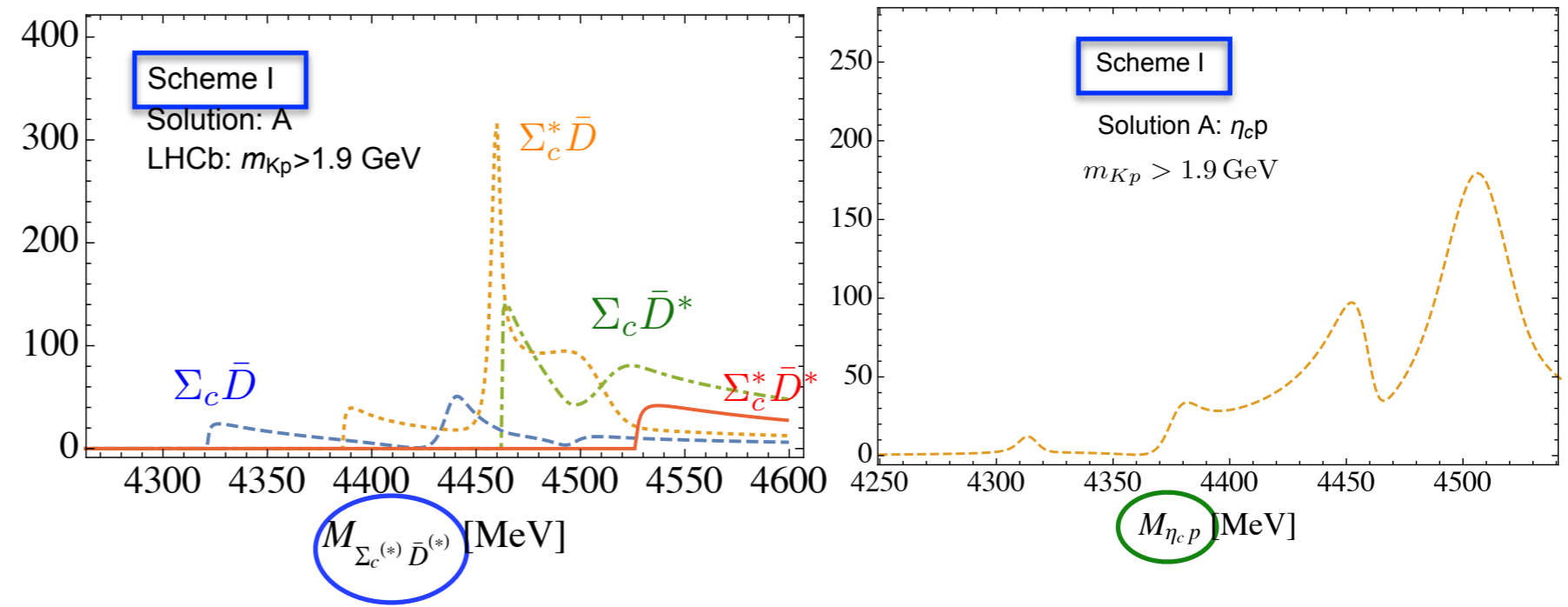
scheme II = contact + OPE

Fit A

Fitted



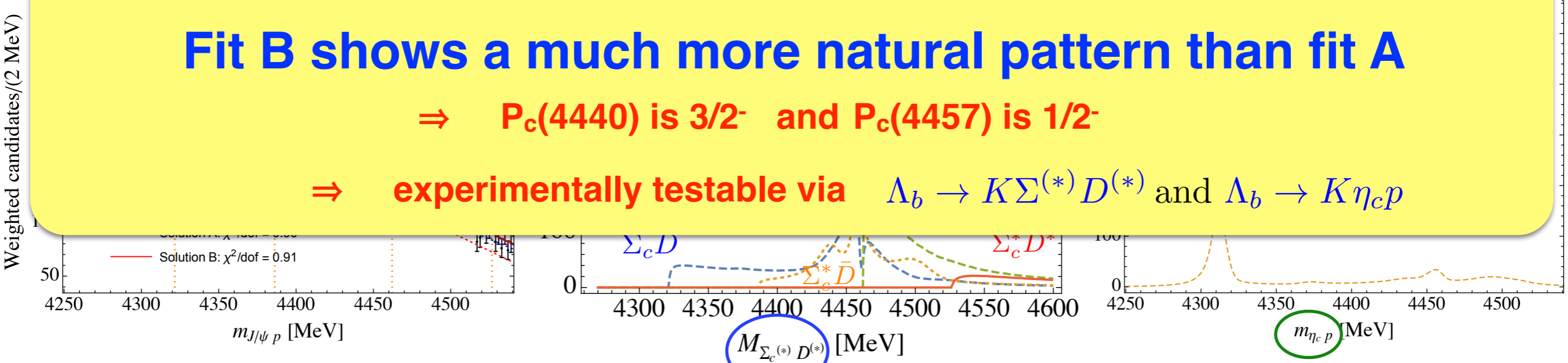
Predicted



Fit B shows a much more natural pattern than fit A

$\Rightarrow P_c(4440)$ is $3/2^-$ and $P_c(4457)$ is $1/2^-$

\Rightarrow experimentally testable via $\Lambda_b \rightarrow K \Sigma^{(*)} D^{(*)}$ and $\Lambda_b \rightarrow K \eta_c p$



The effect from renormalised OPE:

- Qualitatively different results for $\Sigma_c D$ and $\eta_c p$ in schemes I and II
- $\Sigma_c D$: $1/2^- P_c(4440)$ in S-wave in scheme I vs $3/2^- P_c(4457)$ in D-wave in scheme II

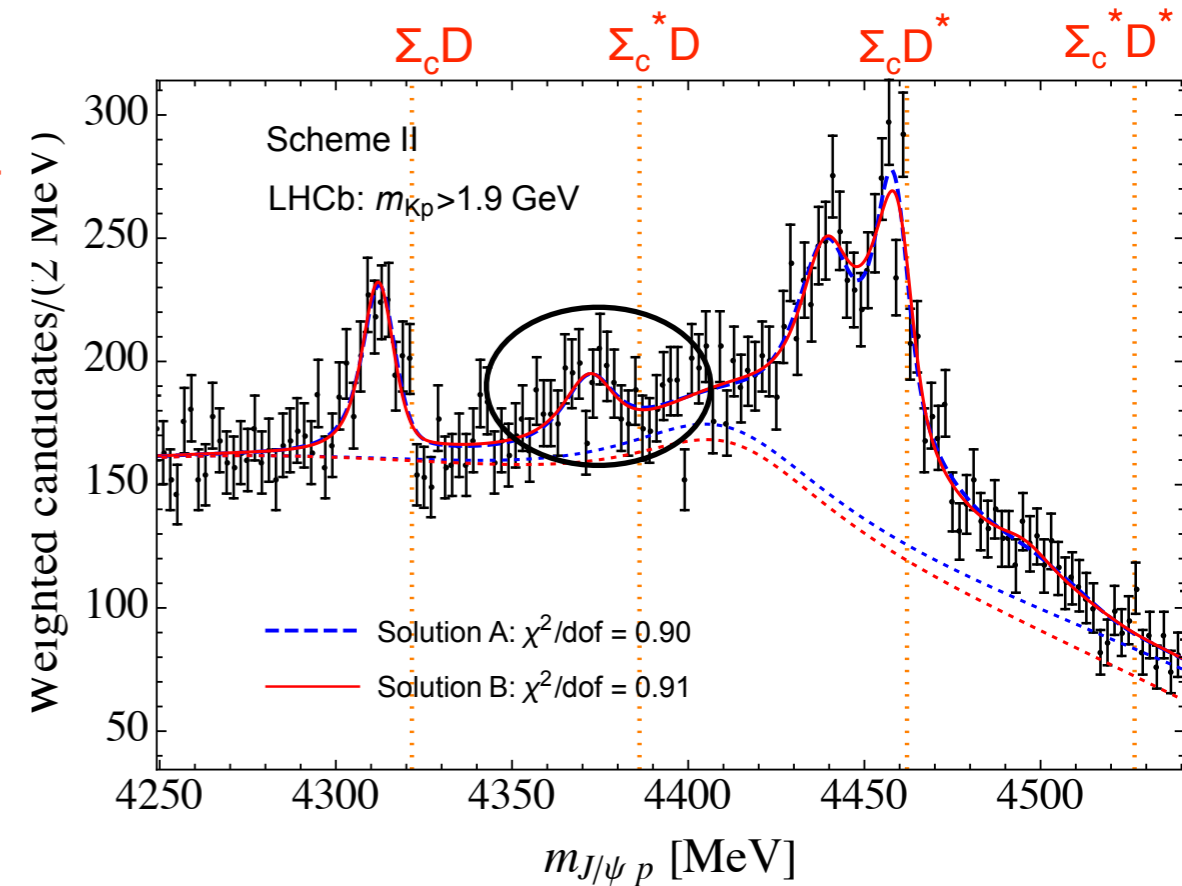
Summary and Outlook

- A coupled-channel analysis of $\Lambda_b \rightarrow K P_c \rightarrow K J/\Psi p \Rightarrow P_c$ states as $\Sigma_c^{(*)} \bar{D}^{(*)}$ quasi-bound states

- A new $P_c(4380)$ as $\Sigma_c^* D$ $3/2^-$ is already in current data

- Testable predictions for spectra

$$\Lambda_b \rightarrow K \Sigma^{(*)} \bar{D}^{(*)} \text{ and } \Lambda_b \rightarrow K \eta_c p$$



- | | | | |
|--------|-------------|-------------|----------------|
| | $P_c(4440)$ | $P_c(4457)$ | $\Sigma_c D^*$ |
| Fit A: | $1/2^-$ | $3/2^-$ | |
| Fit B: | $3/2^-$ | $1/2^-$ | |

 from fits with pions

➡ Data for $\Lambda_b \rightarrow K$ final, final = $\Sigma_c^{(*)} \bar{D}^{(*)}$, $\eta_c p$ and $\Lambda_c \bar{D}^{(*)}$ are needed
 $\Rightarrow J/\Psi p$ data alone are not enough to constraint $\Lambda_c \bar{D}^{(*)}$ interactions

➡ Other data, e.g., $J/\Psi p$ photoproduction: sensitivity to production process